40th postdoc/staff lecture series on cosmology, July 24 2025

Axion birefringence: probing ultra-light particles with polarized light

Patricia Diego Palazuelos

1. Axionlike particles
   - 1.1 Definition
   - 1.2 Misalignment mechanism
     - 1.2.1 Pre- vs post-inflationary scenarios
   - 1.3 Equations of motion and state
   - 1.4 Observational and experimental searches
     - 1.4.1 Laboratory experiments
     - 1.4.2 Cosmology and astrophysics
       - 1.4.2.1 Gravitational interactions
       - 1.4.2.2 Non-gravitational interactions
2. Axion birefringence
   - 2.1 Covariant formulation of electromagnetism
   - 2.2 Chern-Simons coupling to axions
   - 2.3 Propagation of electromagnetic waves
3. Axion birefringence phenomenology
   - 3.1 Phenomenology of isotropic β
   - 3.2 Phenomenology of anisotropic β
4. Probes for axion birefringence
   - 4.1 Polarization primer
   - 4.2 Cosmic microwave background
     - 4.2.1 Isotropic β, axion dark energy
     - 4.2.2 Isotropic β, intermediate masses
     - 4.2.3 Isotropic β, axion dark matter

4.2.4 Anisotropic β

4.3 Radio galaxies

4.4 Protoplanetary disk

4.5 Time delays between strongly lensed images

4.6 Black hole polarimetry

4.7 Pulsars

4.8 Laboratory experiments

1. Axionlike particles

1.1 Definition

See reviews
- Marsh 2016 [arXiv: 1510.07633]
- Ferreira 2021 [arXiv: 2005.03254]
- O'Hare 2024 [arXiv: 2403.17697]

Axionlike particles (ALP) englobe a variety of light, feebly interacting bosons appearing in high-energy physics theories related to CP violation in the standard model, supersymmetry, and theories with extra dimensions, including string theories.
ALP can live in a very broad parameter space of mass (m_ϕ) and coupling to photons ($g_{\phi\gamma\gamma}$). Only the QCD axion is forced to follow a certain relation between m_ϕ and $g_{\phi\gamma\gamma}$ to ensure that it solves the strong CP problem.

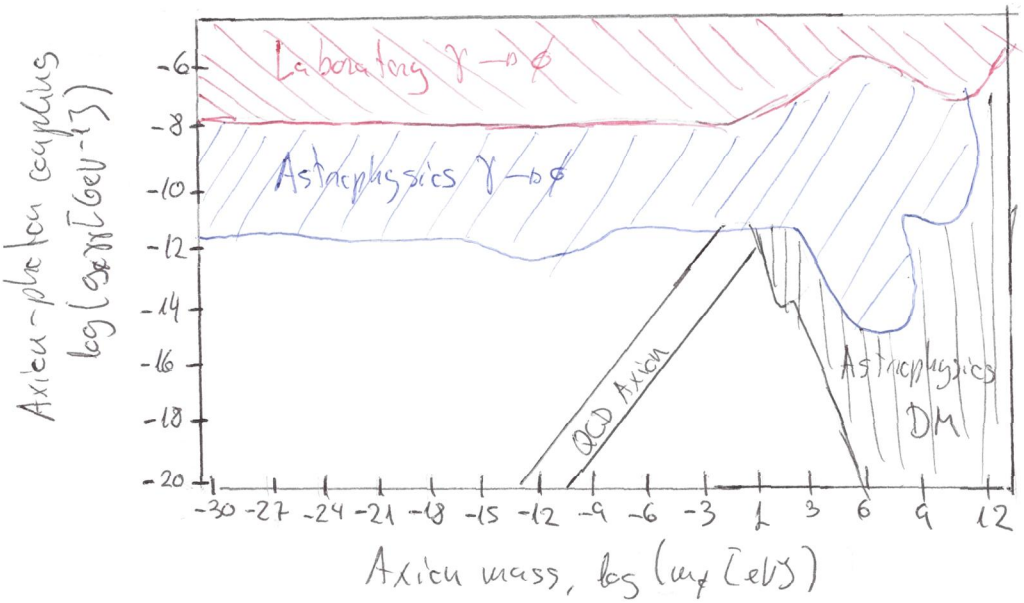

See updated constraints at Ciara O'Hare's GitHub
cajohare/AxionLimits
DOI 10.5281/zenodo.3932430

Ultra-light ALP are a well motivated candidate for dark matter (DM) since they solve the small-scale crisis by suppressing the formation of low mass halos and leading to density cores in the form of solitons

Small-scale crisis
- Missing satellites problem: cold dark matter (CDM) predicts more small Milky Way satellites than observed
- Too-big-to-fail problem: CDM predicts more massive satellites that should contain stars than are observed
- Cusp-core problem: many observed low-mass systems contain flat central density profiles, not Navarro-Frenk-White (NFW) cusps

Important properties of ALP to keep in mind:

- Described by a pseudoscalar field, $\phi(-\hat{n}) = -\phi(\hat{n})$
- Characterized by the axion mass, m_ϕ, and the axion decay constant setting the energy scale of the symmetry breaking, f_ϕ
- The typical axion potential $V(\phi) \propto [1 - \cos(\phi/f_\phi)]$ is approximated by $V(\phi) \simeq \frac{1}{2} m_\phi^2 \phi^2$ around its minimum
- They have a non-thermal production mechanism => misalignment mechanism
- ALP perturbations experience a scale-dependent growth. Axion DM differs from CDM on scales below the axion Jeans scale

Jeans scale	scale where density and pressure are in equilibrium $4\pi G \rho_\phi = K^2 c_s^2$

Going forward, I will use "axion" to refer to all ALP and specify when talking about the QCD axion

1.2 Misalignment mechanism

Axions are pseudo-Nambu Goldstone bosons resulting from the spontaneous symmetry breaking of a global U(1) symmetry described by the complex scalar field

$$\Psi = v e^{i\phi/f_\phi}$$

f_ϕ: energy scale of the spontaneous symmetry breaking

$\theta = \phi/f_\phi$: misalignment angle

When the symmetry is broken, the massive radial component v is fixed at the vacuum expectation value $v_{SSB} = f_\phi/\sqrt{2}$. There is a continuous set of minima with ground state $\Psi = v_{SSB} e^{i\theta}$ corresponding to all possible phases in the circle.

The pseudo-Goldstone boson ϕ is invariant under shift symmetry, inherited from the U(1) symmetry of the complex scalar field.

Non-perturbative effects, e.g., arising from instantons on string theory models, can induce a potential that then breaks the shift symmetry (although softly), which leads to a residual discrete symmetry. This potential gives mass to the axion and has the form

$$V(\phi) = \Lambda_\phi^4 \left[1 - \cos\left(\frac{\phi}{f_\phi}\right)\right]$$

Λ_ϕ: energy scale of the explicit symmetry breaking

Instanton // Tunnelling solutions that connect the landscape of topologically inequivalent vacua. Their effect is temperature dependent

Since the spontaneous symmetry breaking scale f_ϕ is usually much higher than the explicit symmetry breaking, the mass and self-interaction coupling constant are very small

$$m_\phi = \Lambda_\phi^2 / f_\phi \qquad g_{\phi\phi} = -\Lambda_\phi^4 / f_\phi^4$$

Interactions with standard model particles are suppressed by powers of f_ϕ

For small field values, $\phi << f_\phi$, the potential can be approximated by

$$V(\phi) \simeq \frac{1}{2} m_\phi^2 \phi^2 + \frac{g_{\phi\phi}}{4!} \phi^4 + \dots$$

For the QCD axion, the symmetry broken is the chiral global U(1)pq, the Peccei-Quinn symmetry, which is later explicitly broken at Taco temperature

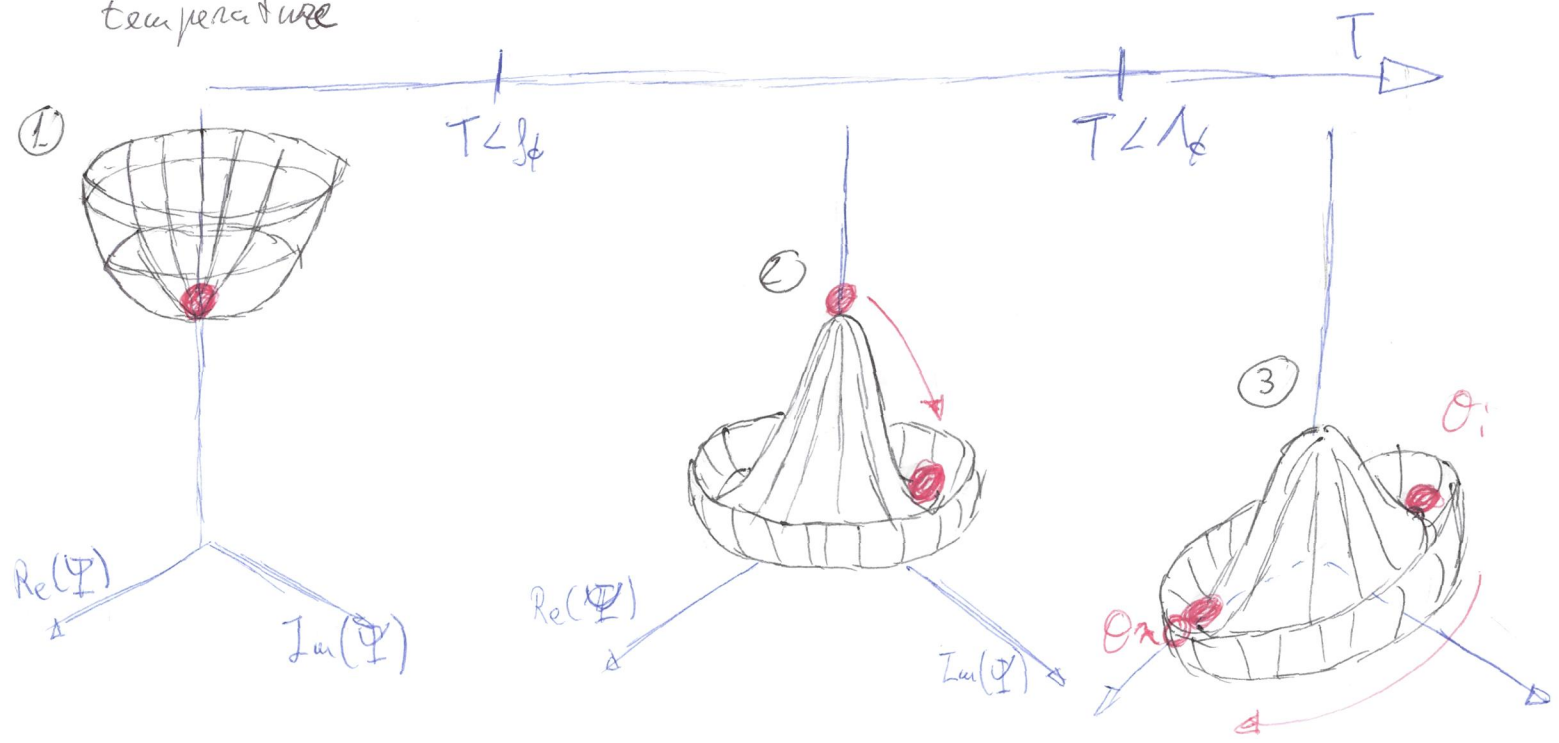

① The axion appears as a massless angular degree of freedom when the U(1) symmetry is spontaneously broken at $T \lesssim f_a$

② The axion acquires a mass $m_a = \Lambda_a^2 / f_a$ when the shift symmetry is explicitly broken at Λ_a

③ The initial angle θ_i that was chosen at $T \sim f_a$ is expected to be misaligned from the $\theta = 0$ where the axion resides today

1.2.1 Pre- vs post-inflationary scenarios

Depending on whether the symmetry breaking happened before or after inflation, we will have two different scenarios

Post-inflationary scenario

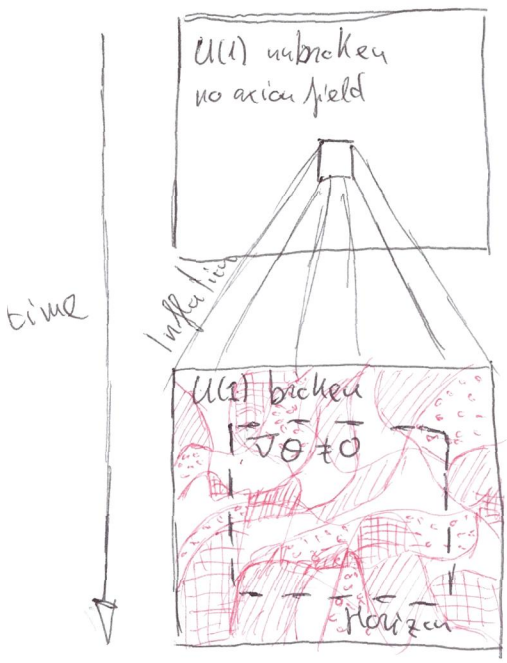

Different regions take different continuous values of θ, with $\langle \theta^2 \rangle \approx \left(\frac{\pi}{\sqrt{3}}\right)^2$ within the horizon

- In each Hubble patch, a random value of θ is chosen from a uniform distribution on $[-\pi, \pi]$
- θ fluctuations are non-adiabatic and not scale invariant, giving rise to axion miniclusters
- Presence of topological defects like domain walls and cosmic string networks

Pre-inflationary scenario

- The rapid expansion during inflation dilutes all phase transition relics away and stretches out patches of θ s.t. that our current Hubble volume has a uniform θ everywhere
- Small fluctuations in θ generate both adiabatic and isocurvature modes

Approximately $\langle\theta^2\rangle \approx$ constant within the horizon

1.3 Equations of motion and state

Around the minimum of the potential, $V(\phi) \approx \frac{1}{2} m_\phi^2 \phi^2$, the background evolution of the axion field is given by the Klein-Gordon equation

$$\ddot{\bar{\phi}} + 3H\dot{\bar{\phi}} + m_\phi^2 \bar{\phi} = 0$$

$\dot{x} = \frac{\partial x}{\partial t}$

The background energy density and pressure are

$$\bar{\rho}_\phi = \frac{1}{2}\dot{\bar{\phi}}^2 + \frac{1}{2} m_\phi^2 \bar{\phi}^2 \qquad \bar{P}_\phi = \frac{1}{2}\dot{\bar{\phi}}^2 - \frac{1}{2} m_\phi^2 \bar{\phi}^2$$

Solving the Klein-Gordon equation

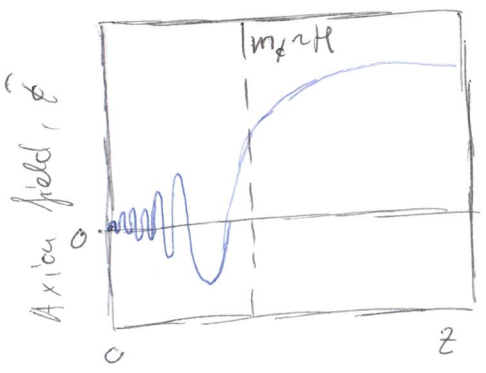

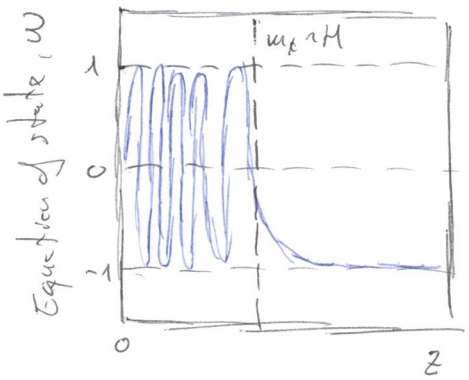

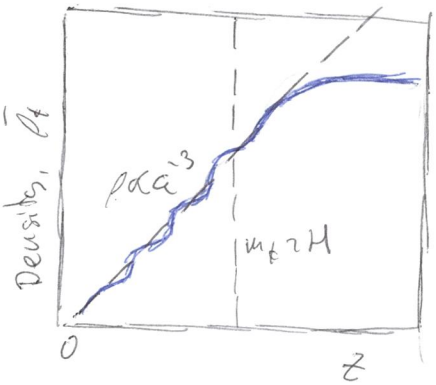

At early times when $H > m_\phi$, $\bar{\phi}$ is overdamped and frozen at its initial value by Hubble friction. The equation of state is $w = -1$, with axions behaving like the fluid responsible for dark energy (DE) or even inflation.

➡ Axions with $m_\phi \lesssim H_0 \sim 10^{-33}$ eV have only recently started evolving and are thus suitable candidates for DE.

Later, when $H < m_\phi$, $\bar{\phi}$ is underdamped and $\phi \propto \cos(m_\phi t + \delta)$ oscillations begin. The equation of state oscillates around $\langle w \rangle = 0$ and the energy density scales as $\bar{\rho}_\phi \propto a^{-3}$, with axions behaving like ordinary matter.

➡ Axions with $m_\phi \gtrsim H(a_{eq}) \sim 10^{-28}$ eV begin oscillating in the radiation dominated era and are thus suitable candidates for DM.

1.4 Observational and experimental searches

Non-exhaustive list covering some of the main observables

1.4.1 Laboratory experiments

Primakoff effect

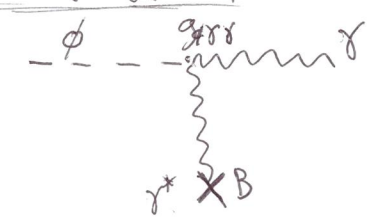

Axion-photon conversion in the presence of a strong magnetic field

Haloscopes

Resonant microwave cavities designed to detect the weak conversion of DM axions into microwave photons in the presence of a strong magnetic field

e.g. ADMX Goodman+2025 [arXiv:2408.15227]
ABRACADABRA Salemi+2021 [arXiv:2102.06727]
RADES Ahyoune+2025 [arXiv:2403.07790]
CAPP Sungjae+2024 [arXiv:2403.13390]
QUAX Rettaroli+2024 [arXiv:2402.19063]

HAYSTAC Bai + 2025 [arXiv: 2409.08998]

ORGAN Quiskamp + 2025 [arXiv: 2407.18586]

CADEX Aja + 2022 [arXiv: 2206.02980]

DM-Radio Brouwer + 2022 [arXiv: 2204.13781]

MADMAX Arg dos Santos Garcia + 2025 [arXiv: 2409.11777]

Helioscopes

Telescopes focusing the soft X-ray photons produced when the axions originated in the Sun by the Primakoff effect interact with a strong magnetic field

e.g. (baby)IAXO IAXO collaboration 2025 [arXiv: 2411.13915]
Armengaud + 2019 [arXiv: 1904.09155]

CAST Altenmüller + 2024 [arXiv: 2406.16840]

Light shining through a wall

Setting: two vacuum chambers permeated by a strong transverse magnetic field and separated by an optical absorber

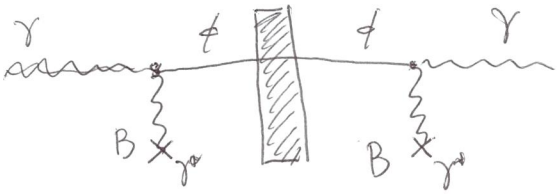

Goal: potentially catch the photons that appear on the other side of the wall after a double axion-photon conversion within the strong magnetic field

e.g. ALPS Ehret + 2010 [arXiv: 1004.1313]
OSQAR Ballou + 2015 [arXiv: 1506.08082]

Colliders, accelerators, and beam dumps

e.g.

ATLAS Atlas Collaboration 2022 [arXiv: 2008.05355]

CMS Sirunyan + 2019 [arXiv: 1810.04602]

Belle Ablikim + 2024 [arXiv: 2409.04640]

BaBar Dolan + 2017 [arXiv: 1709.00009]

OPAL Knapen + 2017 [arXiv: 1607.06083]

DAMIC Chavarria + 2015 [arXiv: 1607.03477]

detect standard model particle recoils resulting from interactions with axions using CCDs

CASPEr Garcon + 2018 [arXiv: 1706.05312]

exploit the spin dependence of axion-nucleon couplings to detect these interactions by searching for spin precession using nuclear magnetic resonance techniques

1.4.2 Cosmology & astrophysics

1.4.2.1 Gravitational interactions

Primary cosmic microwave background (CMB) anisotropies

Axions affect the position and height of acoustic peaks and the Sachs-Wolfe plateau in the CMB TT angular power spectrum as they can change the expansion rate and relative matter-to-radiation density at different times depending on their mass

Matter power spectrum

Axions affect both the expansion rate (through $\mathcal{H}(a)$) and the growth of structure (through the transfer and growth functions).
Compared to CDM, axions cause a suppression of power due to the the axion Jeans scale and require a scale-dependent bias factor, $b(k)$, to capture their scale-dependent clustering.

The combination of these probes provides constraints on the fraction of DM that is allowed to take the form of axions

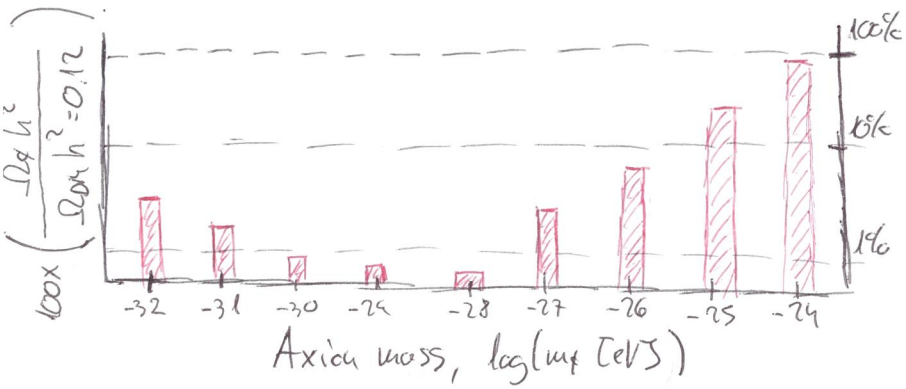

95% upper limits on the fraction of DM in the form of axions inferred from BOSS galaxy clustering and Planck 2018 CMB

Rogers + 2023 [arXiv: 2301.08361]

Isocurvature perturbations

Axions produced in the pre-inflationary scenario lead to isocurvature modes. The absence of isocurvature perturbations constraints the energy scale of the axion symmetry breaking.

The halo mass function (HMF)

HMF: number density of DM halos per mass interval as a function of redshift.

Ultra-light axions dramatically suppress halo formation compared to CDM at low halo masses and at high redshifts

This has important consequences for the epoch of reionization. The cut off in the HMF delays the formation of the first galaxies, thus reionization occurs at lower redshifts than in CDM. Once collapse starts, structure builds up far rapidly than for CDM, and reionization completes in a smaller redshift window.

Halo density profile

Deviation from the NFW profile due to the wavelike effects of ultra-light axions. There is granularity and a smoothing of the central cusp, returning to NFW when the density is smoothed over many Jeans scales.

$$\rho_{NFW}(r) = \frac{\rho_0}{\frac{r}{R_s}\left(1+\frac{r}{R_s}\right)^2}$$

where the scale radius is defined with respect to the virial radius

$R_{vir} = c\, R_s$

$$\rho_{sol}(r) = \frac{\rho_0}{\left[1+\left(\frac{r}{R_{sol}}\right)^2\right]^8}$$

with

$$R_{sol} = 22\left(\frac{\rho_0}{\rho_{crit}}\right)^{-1/4}\left(\frac{m_a}{10^{-22}\,eV}\right)^{-1/2} \text{Kpc}$$

Black hole superradiance

When the Compton wavelength of axions is of the same order as the size of a rotating black hole (BH), axions are expected to form a dense cloud near the event horizon through the superradiance mechanism

Brito+ 2015 [arXiv: 1501.06570]

This cloud eventually radiates away the energy extracted from the BH, e.g., in the form of gravitational waves

Oscillations in pulsar timing

The rapid oscillations in local axion pressure induce oscillations of the gravitational potential that, in turn, produce an oscillating time delay in the arrival time of pulsar signals with frequency $2m_a$.

1.4.2.2 Non-gravitational interactions

(Early time) energy injection

Heavier axions can be unstable on cosmological timescales and will decay to standard model particles (or light dark sector particles). The decay of such a population of axions injects additional relativistic energy into the Universe.

The presence and later decay of axions in the early Universe can change the effective number of relativistic species, N_{eff}, and the baryon-to-photon ratio, $\eta_b = n_b/n_\gamma$, at different times in cosmic history, impacting CMB anisotropies and the relic abundance of light elements.

Energy injection at different epochs can change the shape of the CMB frequency spectrum such that it is no longer a perfect black body (a.k.a., CMB spectral distortions)

Stellar astrophysics

Axions provide a cooling mechanism for stars and supernovae as the radiated photons are converted into axions in the presence of strong magnetic fields. The observed properties of stars/SNe put limits on how much energy is dissipated through this channel.

- The ratio of horizontal branch stars to red giants in galactic globular clusters is altered by axion-photon conversion inside the stars
- Energy loss in globular cluster stars and white dwarfs sets limits on the axion-electron coupling

- The duration of the neutrino burst from SN 1987a can be used to constrain the axion-nucleon interaction. If axions interact strongly enough with nuclei, the axion emission via nucleon bremsstrahlung is a more efficient energy-loss channel than neutrino emission, shortening the observed neutrino burst.
- In a core-collapse supernova, axions would be emitted via the Primakoff process, and eventually convert into γ-rays in the magnetic field of the Milky Way. Therefore, the lack of γ-ray signal in coincidence with the observation of neutrinos emitted from SN 1987a also provides strong bounds on the axion-photon coupling.

Interaction with astrophysical magnetic fields

Axions can convert into photons in the presence of magnetic fields (Primakoff effect). Thus, any astrophysical object with a strong magnetic field can be used as an axion probe.

- Neutron star magnetospheres. The neutron stars' rotating magnetic fields are so strong that their associated electric fields will rip charges off their surfaces, creating a dense plasma of electrons, positrons, and ions around them. Axion-photon conversion will become resonant within the plasma if the plasma frequency matches the axion mass. This process will typically lead to photons in the radio to microwave bands.
- As the X-rays emitted from AGN traverse the magnetized intracluster medium, axion-photon conversion would imprint distortions on the intrinsic AGN spectrum. The absence of observed distortions can be used to put bounds on m_a and $g_{a\gamma\gamma}$
- The hypothesized cosmic axion background with energy around 0.1 to 1 keV would produce an observable excess of X-ray emission when interacting with the magnetic fields of galaxy clusters. In the presence of primordial magnetic fields, this cosmic axion background would also contribute to a diffuse cosmic X-ray background.

And, of course, axion birefringence !!

We will discuss axion birefringence in detail for the rest of the lecture

In the absence of an external magnetic field, we simply have birefringence, i.e., rotation with no absorption.
In the presence of a magnetic field, there is absorption of one polarization state, i.e., dichroism.

2. Axion birefringence

Heaviside units ($\epsilon_0 = \mu_0 = 1$) & $c = 1$

Minkowski spacetime $\eta_{\mu\nu} = (-1, 1, 1, 1)$

with $x^\mu = (x^0, x^i)$; $\partial_\mu = \frac{\partial}{\partial x^\mu} = \left(\frac{\partial}{\partial t}, \vec{\nabla}\right)$ & $\partial^\mu = \left(-\frac{\partial}{\partial t}, \vec{\nabla}\right)$

2.1 Covariant formulation of electromagnetism

Vector potential $A_\mu = (-\varphi, \vec{A})$

$\star$ such that $\vec{E} = -\vec{\nabla}\varphi - \dot{\vec{A}}$ & $\vec{B} = \vec{\nabla} \times \vec{A}$

In addition, $j^\mu = (\rho, \vec{J})$

Antisymmetric field strength tensor

$$F_{\mu\nu} = \partial_\mu A_\nu - \partial_\nu A_\mu = \begin{pmatrix} 0 & -E_x & -E_y & -E_z \\ E_x & 0 & B_z & -B_y \\ E_y & -B_z & 0 & B_x \\ E_z & B_y & -B_x & 0 \end{pmatrix}$$

Dual field strength tensor

$$\tilde{F}^{\mu\nu} = \frac{1}{2} \epsilon^{\mu\nu\alpha\beta} F_{\alpha\beta} = \begin{pmatrix} 0 & B_x & B_y & B_z \\ -B_x & 0 & -E_z & E_y \\ -B_y & E_z & 0 & -E_x \\ -B_z & -E_y & E_x & 0 \end{pmatrix}$$

($\epsilon^{\mu\nu\alpha\beta}$: Levi-Civita symbol)

One set of Maxwell's equations is automatically given by the definition of $F_{\mu\nu}$

$$\partial_\nu \tilde{F}^{\mu\nu} = \partial_\nu \left[\frac{1}{2} \epsilon^{\mu\nu\alpha\beta} (\partial_\alpha A_\beta - \partial_\beta A_\alpha)\right] = \epsilon^{\mu\nu\alpha\beta} \partial_\nu \partial_\alpha A_\beta = 0 \Rightarrow \boxed{\partial_\nu \tilde{F}^{\mu\nu} = 0}$$

Action that gives Maxwell's equations

$$I = -\frac{1}{4} \int d^4x \, F_{\mu\nu} F^{\mu\nu} + \int d^4x \, A_\mu j^\mu \quad \text{where } d^4x = dt \, d^3\vec{x}$$

Action must remain stationary under small variations of A_μ

$$\delta I = -\frac{1}{4} \int d^4x \, \underbrace{\delta(F_{\mu\nu} F^{\mu\nu})}_{2 F^{\mu\nu} \delta F_{\mu\nu} = -4 F^{\mu\nu} \partial_\nu (\delta A_\mu)} + \int d^4x (\delta A_\mu) j^\mu$$

integrating by parts

$$= \int d^4x \left[F^{\mu\nu} \partial_\nu (\delta A_\mu) + (\delta A_\mu) j^\mu\right]$$

$$= \int d^4x \left[-\partial_\nu F^{\mu\nu} + j^\mu\right] \delta A_\mu = 0 \Rightarrow \boxed{\partial_\nu F^{\mu\nu} = j^\mu}$$

the other set of Maxwell's equations

The classical equations are derived from the covariant formulation

$\partial_\nu F^{\mu\nu} = j^\mu$ $\begin{cases} \partial_\mu F^{\mu 0} = j^0 \rightarrow \nabla \cdot \vec{E} = \rho & \text{Gauss' law} \\ \partial_\mu F^{\mu i} = j^i \rightarrow \nabla \times \vec{B} - \dot{\vec{E}} = \vec{J} & \text{Ampère-Maxwell law} \end{cases}$

$\partial_\nu \tilde{F}^{\mu\nu} = 0$, which contains the Bianchi identity

$\partial_\mu F^{\lambda\nu} + \partial_\nu F^{\mu\lambda} + \partial_\lambda F^{\mu\nu} = 0$

- $\mu = 1, \nu = 2, \lambda = 3$
  $\rightarrow \nabla \cdot \vec{B} = 0$ Gauss' law for magnetism
- $\mu = 0, \nu = 2, \lambda = 3$
  $\rightarrow \nabla \times \vec{E} + \dot{\vec{B}} = 0$ Faraday's law

2.2 Chern-Simons coupling to axions

Ni 1977 — Turner & Widrow 1988
Sikivie 1983 — Carroll, Field, Jackiw 1990

Chern-Simons action

$$I_{CS} = -\frac{1}{4}\alpha \int d^4x\, \theta F_{\mu\nu}\tilde{F}^{\mu\nu} \quad \text{with } \alpha \text{, dimensionless constant}$$

$F_{\mu\nu}\tilde{F}^{\mu\nu} = 2\partial_\mu(A_\nu \tilde{F}^{\mu\nu})$ (integration by parts)

θ, dimensionless pseudoscalar field, like that of axions, $\theta = a/f_a$

$$= \frac{1}{2}\alpha \int d^4x\, (\partial_\mu \theta) A_\nu \tilde{F}^{\mu\nu}$$

Special case of the Chern-Simons term $p_\mu A_\nu \tilde{F}^{\mu\nu}$

To ensure the EM action remains invariant under the gauge transformation $A_\nu \rightarrow A_\nu + \partial_\nu f$, p_μ must fulfill $\partial_\nu p_\mu = \partial_\mu p_\nu$, therefore it must be either

- A constant vector introducing a preferred direction in spacetime and violation of Lorentz invariance, $\partial_\nu p_\mu = 0$
- Like in our case, the gradient of a dynamical pseudoscalar field, $p_\mu = \partial_\mu \theta$. θ must be a pseudoscalar to ensure the parity invariance of the total action since $F_{\mu\nu}\tilde{F}^{\mu\nu} = -4\vec{B}\cdot\vec{E}$ is a pseudoscalar and changes sign under parity transformation

Adding this term to the action

$$I + I_{CS} = -\frac{1}{4}\int d^4x \left(F_{\mu\nu}F^{\mu\nu} + \alpha\theta F_{\mu\nu}\tilde{F}^{\mu\nu}\right) + \int d^4x\, A_\mu j^\mu$$

will modify Maxwell's equations to

$$\delta I = \int d^4x \, (F^{\mu\nu} + \alpha\theta \tilde{F}^{\mu\nu}) \partial_\nu (\delta A_\mu) + \int d^4x \, (\delta A_\mu) j^\mu$$

integrating by parts →

$$\int d^4x \left[-\partial_\nu (F^{\mu\nu} + \alpha\theta \tilde{F}^{\mu\nu}) + j^\mu \right] \delta A_\mu = 0$$

$$\boxed{\partial_\nu F^{\mu\nu} + \alpha (\partial_\nu \theta) \tilde{F}^{\mu\nu} = j^\mu}$$

2.3 Propagation of electromagnetic waves

Classical electromagnetism

$\partial_\nu F^{\mu\nu} = 0$ Maxwell's equations in vacuum

↳ $-\Box A^\mu + \eta^{\mu\alpha} \partial_\alpha (\partial_\nu A^\nu) = 0$ where $\Box = \eta^{\alpha\beta} \partial_\alpha \partial_\beta = -\frac{\partial^2}{\partial t^2} + \nabla^2$

$A^\mu = \eta^{\mu\alpha} A_\alpha = (\varphi, \vec{A})$

In Lorentz + Coulomb gauge conditions

$\partial_\nu A^\nu = 0$ & $A^0 = \varphi = 0$

⇒ $\boxed{-\Box A^\mu = \ddot{\vec{A}} - \nabla^2 \vec{A} = 0}$ wave equation

Going to Fourier space

$$A(t, \vec{x}) = \frac{1}{(2\pi)^{3/2}} \int d^3\vec{k} \; \vec{A}_k(t) \, e^{i\vec{k}\cdot\vec{x}}$$

with EM waves propagating in the direction of $\vec{k}$.

The change in $\vec{A}_k$ is perpendicular to $\vec{k}$ so that in the Coulomb gauge

$$\nabla \cdot \vec{A}(t, \vec{x}) = 0 \rightarrow \vec{k} \cdot \vec{A}_k(t) = 0,$$

making the wave eq. in Fourier space

$$\ddot{\vec{A}}_k + k^2 \vec{A}_k = 0$$

Choosing $\vec{k}$ to be on the $\hat{z}$ axis, we can define a helicity basis of $\lambda = \pm 1$ states that are given for each Fourier mode by

$$A_\pm = \frac{A_k^{(x)} \mp i A_k^{(y)}}{\sqrt{2}}$$

In this basis, the wave eq. is $\ddot{A}_\pm + k^2 A_\pm = 0$!!

Both helicity states propagate at the same phase velocity, $\omega_\pm = k$ (or $\omega_\pm = ck$ bringing back factors of c).

EM + Chern-Simons coupling to axions

Carroll, Field, Jackiw 1990
Carroll & Field 1991
Harari & Sikivie 1992

Maxwell's equations in vacuum

$$\partial_\nu F^{\mu\nu} + \alpha (\partial_\nu \theta) \tilde{F}^{\mu\nu} = 0$$

In Lorentz + Coulomb gauge conditions

$$\partial_\nu A^\nu = 0 \;\&\; A^0 = \varphi = 0$$

$$\hookrightarrow -\Box \vec{A}^i + \alpha (\partial_\nu \theta) \tilde{F}^{i\nu} = 0$$

$$\Rightarrow \ddot{\vec{A}} - \vec{\nabla}^2 \vec{A} + \alpha \left[-\dot{\theta} (\vec{\nabla} \times \vec{A}) + (\vec{\nabla}\theta) \times \dot{\vec{A}} \right] = 0$$

Correction to EM wave equation

If axions experience a time-dependent background evolution, $\theta(t, \vec{x}) \to \bar{\theta}(t)$, we find in Fourier space that

$$\ddot{\vec{A}}_k + k^2 \vec{A}_k - i\alpha \dot{\bar{\theta}} (\vec{k} \times \vec{A}) = 0,$$

and projecting into the helicity basis

$$\ddot{A}_\pm + (k^2 \mp k \alpha \dot{\bar{\theta}}) A_\pm = 0$$

!!

$$\Rightarrow \omega_\pm^2 = k^2 \mp k \alpha \dot{\bar{\theta}}$$

For photons we observe today $k^2 \gg k \alpha \dot{\bar{\theta}}$

$$\omega_\pm \simeq k \mp \frac{\alpha}{2} \dot{\bar{\theta}}$$

Parity violation

The equation of motion depends on the handedness

Left- and right-handed circular polarization states propagate at a different phase velocity, introducing a net rotation in the plane of linear polarization

$$\beta = -\frac{1}{2} \int_{t_{emit}}^{t_{obs}} dt (\omega_+ - \omega_-) = \frac{\alpha}{2} \int_{t_{emit}}^{t_{obs}} \dot{\bar{\theta}}\, dt = \frac{\alpha}{2} \left(\bar{\theta}_{obs} - \bar{\theta}_{emit} \right)$$

Birefringence !!

or $\beta = \frac{g_{a\gamma\gamma}}{2} (\bar{\phi}_{obs} - \bar{\phi}_{emit})$ by renaming $\alpha / f_a = g_{a\gamma\gamma}$ as the axion-photon coupling constant

Note that this birefringence rotation is independent of the photon frequency, allowing us to distinguish from other physical processes that rotate the polarization of EM waves

E.g. • Faraday rotation in the presence of magnetic fields ⇝ $\beta \propto \nu^{-2}$

• Quantum gravity effects leading to Lorentz- and CPT-breaking terms in the effective Lagrangian

⇝ $\beta \propto \nu$

Shore 2005 [arXiv: hep-th/0405125]

or $\beta \propto \nu^2$

Myers + 2003 [arXiv: hep-ph/0301124]

Gambini + 1999 [arXiv: gr-qc/9809038]

3. Axion birefringence phenomenology

$$\beta = \frac{g_{a\gamma\gamma}}{2}\left(\phi_{obs} - \phi_{emit}\right)$$

Very diverse phenomenology depending on

- time evolution of axions, $\frac{\partial\phi}{\partial t}$ ⇝ mass of the axion
- spatial distribution of axions
  $\phi(t,\vec{u}) = \bar{\phi}(t) + \delta\phi(t,\vec{u})$ ⇒ $\beta(\vec{u})$ ⇝ formation mechanism

3.1 Phenomenology of isotropic β

Nakatsuka + 2022 [arXiv:2203.08560]

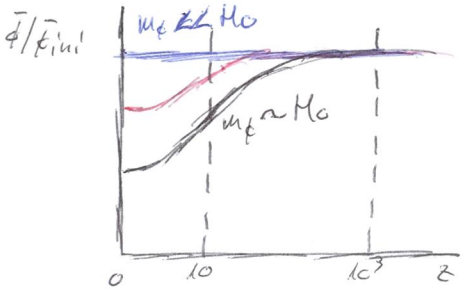

$m_\phi \lesssim H_0 = 10^{-33}$ eV ⇒ axion DE

Need a very long baseline to probe such a small $\Delta\phi$
→ CMB, from $z \simeq 1100$ to $z = 0$

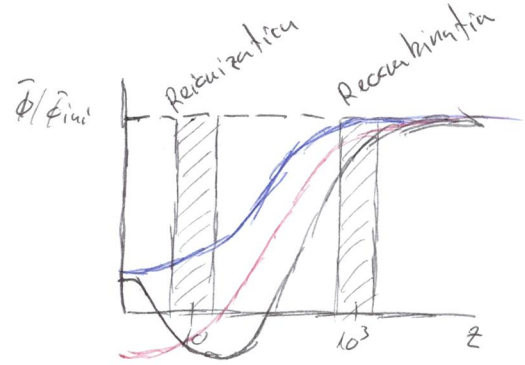

10^{-33} eV $\lesssim m_\phi \lesssim 10^{-28}$ eV intermediate masses

We can observe different β from photons emitted at different z → birefringence tomography

- Cosmological probes: CMB polarization from the epochs of recombination ($z \simeq 1100$) vs reionization ($z \simeq 10$)
- Astrophysical probes: e.g., polarized synchrotron radiation from the jets of radio galaxies

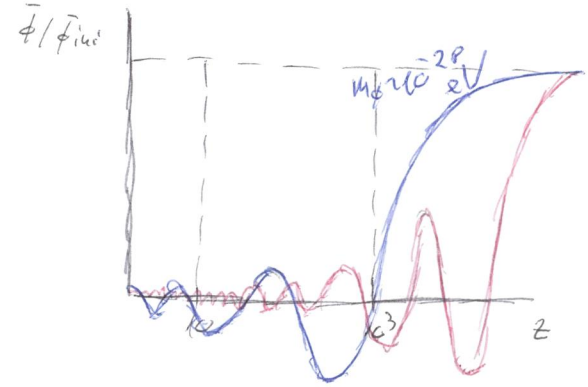

10^{-28} eV $\lesssim m_\phi$ ⇒ axion DM

$\bar{\phi}(t)$ oscillations produce a $\beta(t)$ that oscillates with a period $T \simeq 1\,\mathrm{yr}\,(10^{-22}\,\mathrm{eV}/m_\phi)$

1 yr	$\simeq 10^{-22}$ eV	Astrophysical sources
1 month	$\simeq 10^{-21}$ eV	
1 h	$\simeq 10^{-19}$ eV	Laboratory experiments
1 s	$\simeq 10^{-15}$ eV	
1 ms	$\simeq 10^{-9}$ eV	
1 μs	$\simeq 10^{-6}$ eV	

Human timescales !!

3.2 Phenomenology of anisotropic β

Measure the rotation across the sky

$$\beta(\hat{n}) = \sum_{L=0}^{\infty} \sum_{M=-L}^{L} \beta_{LM} Y_{LM}(\hat{n})$$

to reconstruct the angular power spectrum

$$\langle \beta_{LM} \beta^*_{L'M'} \rangle = \delta_{MM'} \delta_{LL'} C_L^{\beta\beta}$$

Pre-inflationary scenario

As any other field, ϕ will experience quantum fluctuations during inflation, $\delta\phi = \frac{H_I}{2\pi}$, leading to a scale-invariant $P_\phi(k) = \left(\frac{H_I}{2\pi}\right)^2$.

In this case, the birefringence power spectrum is also scale invariant

$$C_L^{\beta\beta} = \frac{2\pi}{L(L+1)} \left(\frac{g_{\phi\gamma\gamma}}{2}\right)^2 \left(\frac{H_I}{2\pi}\right)^2 = \frac{2\pi}{L(L+1)} A_{CB}$$

Current constraints, $A_{CB} < 0.044 \times 10^{-4}$ [rad^2] BICEP/Keck XVII 2023 [arXiv: 2210.08038]

We can also have adiabatic modes that are sourced by curvature fluctuations and will be correlated to primordial density fluctuations

→ $C_L^{\beta T}$, $C_L^{\beta E}$, $C_L^{\beta g}$ Caldwell+ 2011 [arXiv: 1104.1634]
Greco+ 2022 [arXiv: 2202.04584]
Arcari+ 2024 [arXiv: 2407.02144]

Post-inflationary scenario

More complex $P_\phi(k)$ and $C_L^{\beta\beta}$ depending on the properties of topological defects and/or the structure of axion miniclusters

E.g., anisotropic birefringence in a domain wall network Ferreira+2024 [arXiv: 2312.14104]

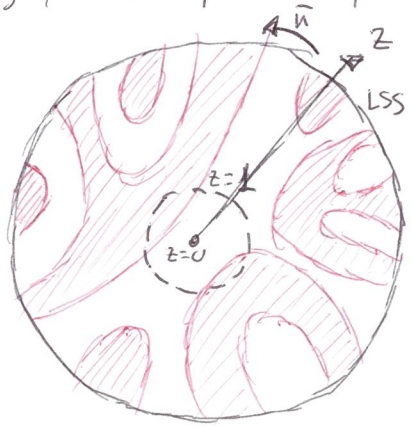

Celestial plot of a domain wall network with two vacua

At the spontaneous symmetry breaking, regions collapsed into different vacua

Photons crossing between regions will see $\Delta\phi$ and experiment β

Topological defects will also radiate gravitational waves!

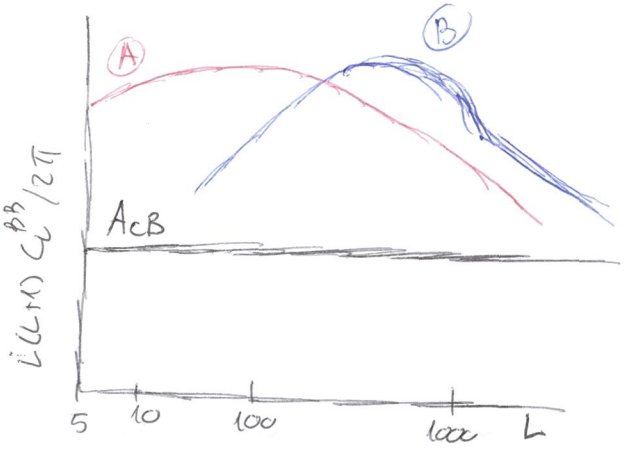

Predictions for C_L^{BB} are very model dependent, but they have distinct features

(A) Long-lived string network from
Jain + 2022 [arXiv: 2208.08391]

(B) Domain wall network from
Ferreira + 2024 [arXiv: 2312.14104]

4. Probes for axion birefringence

Typical masses covered by available / proposed probes

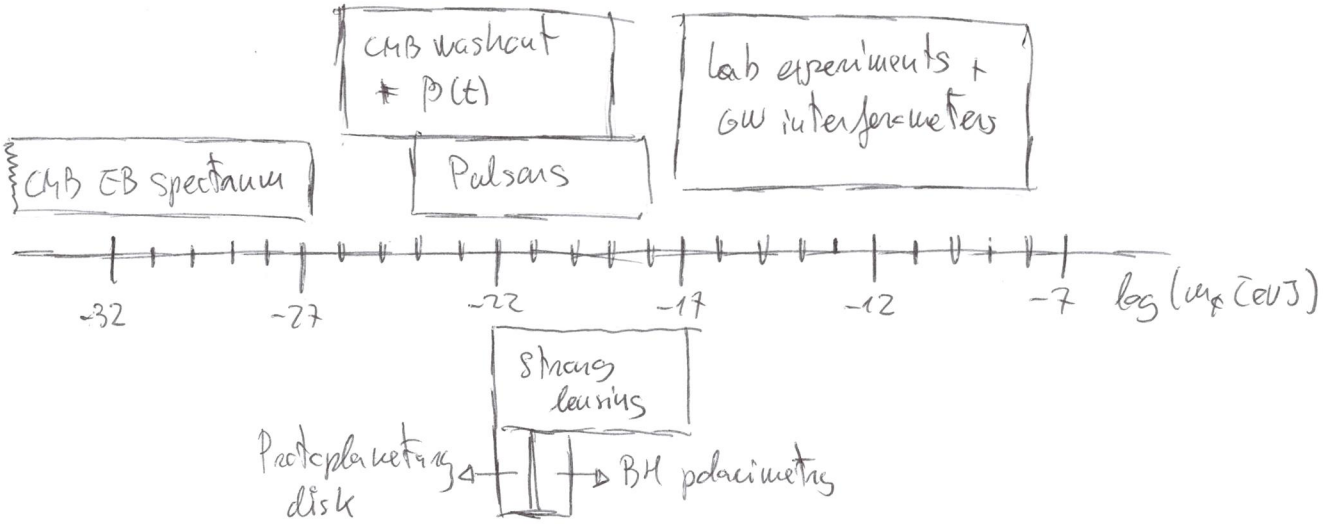

Warning! Depending on the relation between the coherence length of axions across different mass scales and the distance from the observer & the source and physical size of the source, sometimes we will be sensitive to the $\phi(t)$ oscillations on Earth and other times to the $\phi(t)$ oscillations at the source

4.1 Polarization primer | Cabella + 2004 [arXiv: astro-ph/0403392]

Linearly polarized light traveling along the $\hat{z}$ direction

$$E_x = a_x \cos(\omega t) \; ; \quad E_y = a_y \cos(\omega t - \delta)$$

can be described in terms of the Stokes' parameters

$$I = a_x^2 + a_y^2$$

$$Q = a_x^2 - a_y^2$$

$$U = 2 a_x a_y \cos(\delta)$$

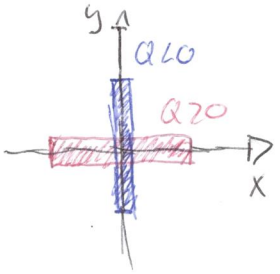

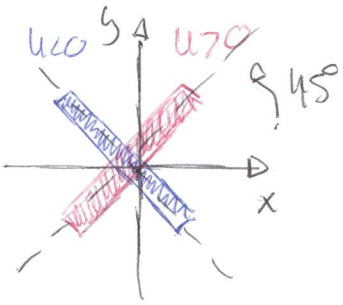

[$V = 2 a_x a_y \sin(\delta)$ for circular polarization]

Q & U define a spin-2 polarization field

$$P_{ab}(\vec{n}) = \frac{1}{\sqrt{2}} \begin{pmatrix} Q(\vec{n}) & \sin(\theta)\, U(\vec{n}) \\ \sin(\theta)\, U(\vec{n}) & -\sin^2(\theta)\, Q(\vec{n}) \end{pmatrix}$$

A β rotation in the plane of linear polarization transforms Stokes' parameters like $(Q \pm iU)(\vec{n}) \longrightarrow e^{\pm i 2\beta} (Q \pm iU)(\vec{n})$, i.e.,

$$Q^{obs}(\hat{u}) = \cos(2\beta)\, Q(\hat{u}) - \sin(2\beta)\, U(\hat{u})$$

$$U^{obs}(\hat{u}) = \sin(2\beta)\, Q(\hat{u}) + \cos(2\beta)\, U(\hat{u})$$

Goal: find astrophysical or cosmological sources of known polarization

Detection and rotation of Q^{obs} & U^{obs} with respect to Q & U

4.2 Cosmic microwave background

Thermal relic of photons last-scattered during the epoch of recombination ($z \simeq 1100$), currently at $T_{CMB} = 2.725\ K$

In the full-sky it is more convenient to decompose the polarization field into its gradient (E) and curl (B) components

$$\nabla^2 E(\hat{u}) = \nabla_a \nabla_b P^{ab}(\hat{u}) \quad \rightarrow \text{independent of coordinate system}$$

$$\nabla^2 B(\hat{u}) = \epsilon_{ac} \nabla_b \nabla_c P^{ab}(\hat{u}) \quad \rightarrow \text{eigenstates of parity}$$

ϵ_{ac}: anti-symmetric tensor; $\nabla_b \nabla_c$: covariant derivatives in the sphere

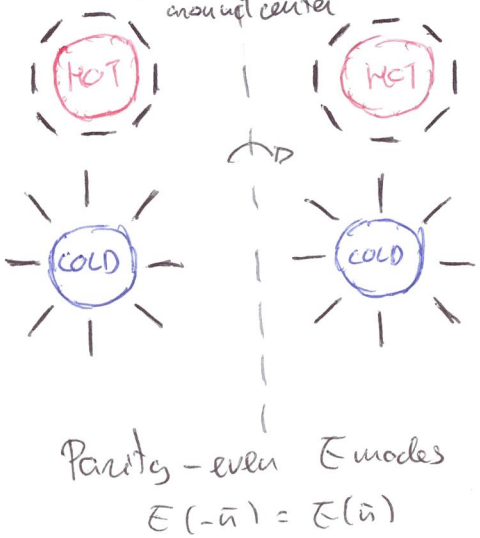

Parity-even E modes

$E(-\hat{u}) = E(\hat{u})$

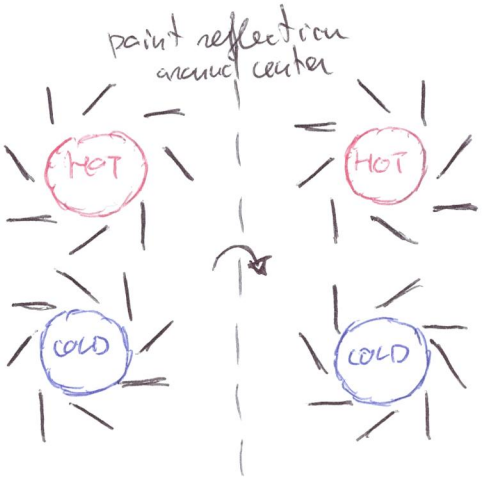

Parity-odd B modes

$B(-\hat{u}) = -B(\hat{u})$

T, E/B decomposition of the full-sky signal into spherical harmonics

$$\langle t_{\ell m}\, t^*_{\ell' m'} \rangle = \delta_{\ell\ell'}\, \delta_{mm'}\, C_\ell^{TT}$$

$$\langle t_{\ell m}\, e^*_{\ell' m'} \rangle = \delta_{\ell\ell'}\, \delta_{mm'}\, C_\ell^{TG}$$

$$\langle e_{\ell m}\, e^*_{\ell' m'} \rangle = \delta_{\ell\ell'}\, \delta_{mm'}\, C_\ell^{EE}$$

$$\langle b_{\ell m}\, b^*_{\ell' m'} \rangle = \delta_{\ell\ell'}\, \delta_{mm'}\, C_\ell^{BB}$$

} parity-even angular power spectra

$\langle a_{\ell m} b_{\ell' m'}^* \rangle = \delta_{\ell\ell'} \delta_{mm'} C_\ell^{TB}$ } parity-odd angular power spectra
$\langle a_{\ell m} b_{\ell' m'}^* \rangle = \delta_{\ell\ell'} \delta_{mm'} C_\ell^{EB}$ } → only not null in the presence of β (assuming no other parity-violating physics)

4.2.1 Isotropic β, axion DE $\quad m_\phi \lesssim 10^{-33}$ eV

All CMB photons (across z and $\hat{n}$) suffer the same β rotation

E^{obs} & B^{obs} rotate into each other

Lue + 1999 [arXiv: astro-ph/9812088]
Feng + 2005 [arXiv: hep-ph/0406264]

$$a_{E,\ell m}^{obs} = \cos(2\beta)\, a_{E,\ell m} - \sin(2\beta)\, a_{B,\ell m}$$
$$a_{B,\ell m}^{obs} = \sin(2\beta)\, a_{E,\ell m} + \cos(2\beta)\, a_{B,\ell m}$$

so that

$$C_\ell^{TT,obs} = C_\ell^{TT}$$
$$C_\ell^{TE,obs} = \cos(2\beta)\, C_\ell^{TE}$$
$$C_\ell^{TB,obs} = \sin(2\beta)\, C_\ell^{TE}$$
$$C_\ell^{EE,obs} = \cos^2(2\beta)\, C_\ell^{EE} + \sin^2(2\beta)\, C_\ell^{BB}$$
$$C_\ell^{BB,obs} = \sin^2(2\beta)\, C_\ell^{EE} + \cos^2(2\beta)\, C_\ell^{BB}$$
$$C_\ell^{EB,obs} = \frac{1}{2}\sin(4\beta)\left(C_\ell^{EE} - C_\ell^{BB}\right)$$

* Focus on EB because it has a higher S/N
  - Fisher information analysis shows that TB has a higher variance
  - TB was useful in noise dominated experiments since T is larger than E

* B modes are sensitive to birefringence
  → confusion between z and β at large angular scales

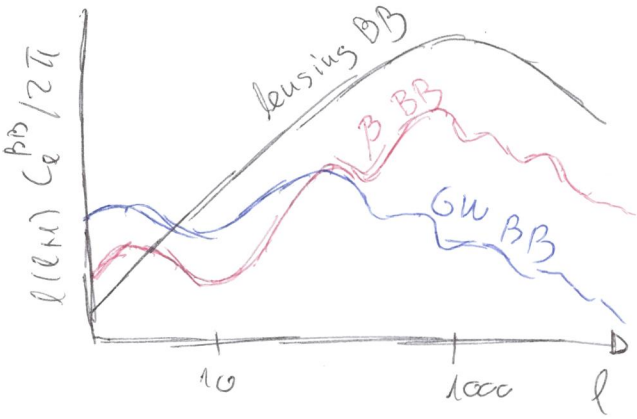

* Smoking gun $C_\ell^{EB} \propto C_\ell^{EE}$

Problem: instrumental systematics !!
In particular, the miscalibration of instrumental polarization angles can introduce spurious EB correlations that mimic this signal

Hint of $\beta \sim 0.20° - 0.35°$ from WMAP + Planck PR4 Eskilt + 2022 [arXiv: 2205.13962] & ACT DR6 Louis + 2025 [arXiv: 2503.14452]

This is my main field of work.

4.2.2 Isotropic β, intermediate masses $\quad 10^{-33}\,eV \lesssim m_\phi \lesssim 10^{-28}\,eV$

CMB polarization is mostly generated during the epoch of recombination ($z_{rec} \simeq 1100$), but we also have a small secondary injection of polarized photons during the epoch of reionization ($z_{reio} \simeq 10$)

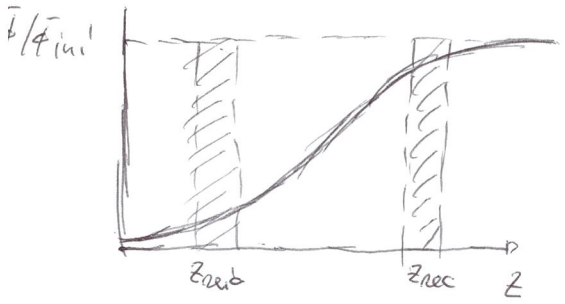

Effective toy model:

$$\beta(z) \begin{cases} \beta_{rec} & \text{for } 10 \lesssim z \\ \beta_{reio} & \text{for } 0 \lesssim z \lesssim 10 \\ 0 & \text{for } z = 0 \end{cases}$$

$$C_\ell^{EB,obs} = \frac{1}{2}\sin(4\beta_{rec})\, C_\ell^{EE,rec} + \frac{1}{2}\sin(4\beta_{reio})\, C_\ell^{EE,reio} + \sin(2\beta_{reio} + 2\beta_{rec})\, C_\ell^{E_{rec}E_{reio}}$$

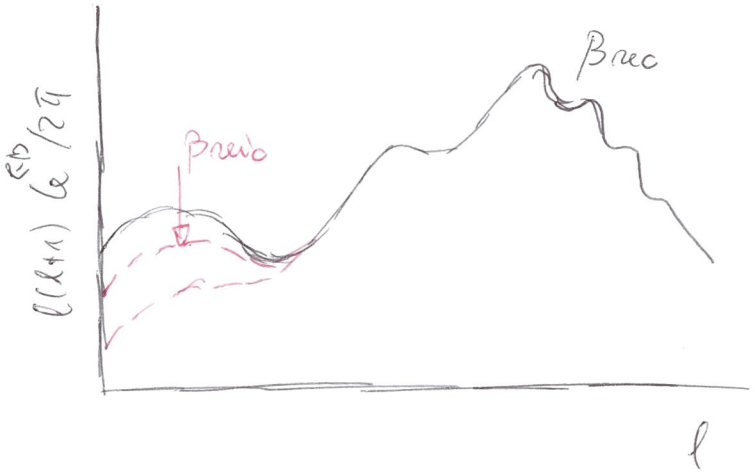

- Small scales (high ℓ) are dominated by photons scattered during recombination → probe β_{rec}
- Large scales (low ℓ) are dominated by photons scattered during reionization → probe β_{reio}

Nakatsuka + 2022 [arXiv: 2203.08560]

We need low ℓ to learn about $\phi(z)$ and distinguish between DE and DM axions → space mission such as LiteBIRD

4.2.3 Isotropic β, axion DM $\quad 10^{-28}\,eV \lesssim m_\phi$

For $m_\phi \gtrsim 10^{-27}\,eV$, $C_\ell^{EB,obs}$ is no longer proportional to C_ℓ^{EE}.

The EB spectrum has a more complex shape since ϕ is already oscillating during recombination. E.g., the acoustic oscillations peaks in EB are shifted with respect to EE.

Namikawa + 2025 [arXiv: 2505.20874]

Fedderke + 2019 [arXiv: 1903.02666]

For higher masses, we start to see the effect of $\beta(t)$

$$(Q \pm iU)_{obs}(\hat{n}) = J_0(g_{\phi\gamma\gamma}\langle\phi\rangle_{LSS}) \; e^{\pm 2i\left[\frac{g_{\phi\gamma\gamma}}{2}\cos(m_\phi t + \delta)\right]} (Q \pm iU)(\hat{n})$$

Washout effect from $\phi(t)$ during recombination

$\beta(t)$ oscillations depending on the local oscillation of $\phi(t)$ $\quad T \sim 1\,\mathrm{yr}\,(10^{-22}\,\mathrm{eV}/m_\phi)$

Washout is a consequence of recombination not being an instantaneous process

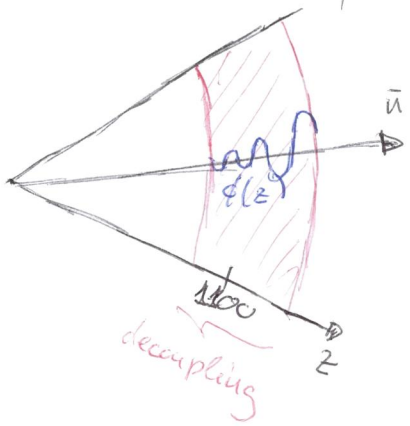

At every direction on the sky, we see CMB photons that were emitted at different times and thus experienced different $\phi(t)$ during recombination

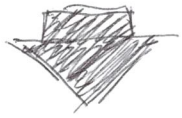

Polarization vectors get rotated by slightly different β

We measure the average of all these superimposed states, leading to a reduction of the total polarization intensity

$$e^{EE}\, J_0(g_{\phi\gamma\gamma}\langle\phi\rangle_{LSS}) \simeq \left[1 - \frac{1}{4}(g_{\phi\gamma\gamma}\langle\phi\rangle_{LSS})^2\right] e^{EE}$$

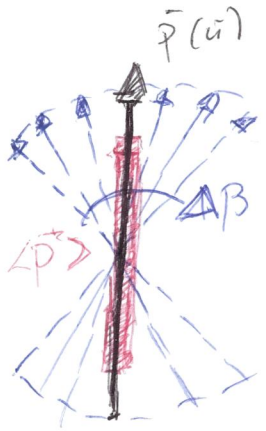

Early SPT-3G data) $\beta(t) \leq 0.07^\circ$ over $1\,\mathrm{day} \leq T \leq 100\,\mathrm{days}$

$$10^{-22}\,\mathrm{eV} \leq m_\phi \leq 10^{-19}\,\mathrm{eV}$$

$$g_{\phi\gamma\gamma} \leq 1.18\times10^{-12}\,\mathrm{GeV}^{-1}\left(m_\phi/10^{-21}\,\mathrm{eV}\right)$$

assuming DM made of one axion species with local density of $0.3\,\mathrm{GeV/cm^3}$ Ferguson + 2022 [arXiv: 2203.16567]

Planck washout)

$$g_{\phi\gamma\gamma} \leq 9.6\times10^{-13}\,\mathrm{GeV}^{-1}\left(\frac{m_\phi}{10^{-21}\,\mathrm{eV}}\right)\left(\kappa\,\frac{\Omega_c h^2}{0.11933}\right)^{-1/2}$$

κ is the fraction of DM in the form of axions at the average redshift of decoupling Fedderke + 2019 [arXiv: 1903.02666]

4.2.4 Anisotropic β

The position-dependent rotation of $\beta(\hat{n})$ introduces higher-order moments and off-diagonal mode couplings in CMB spherical harmonic coefficients

$$(e_{\ell m} \pm i b_{\ell m})^{obs} = (e_{\ell m} \pm i b_{\ell m}) + \sum_{LM} \sum_{\ell' m'} (-1)^m \begin{pmatrix} \ell & L & \ell' \\ -m & M & m' \end{pmatrix} W^{\pm}_{\ell L \ell'} (e_{\ell' m'} \pm i b_{\ell' m'}) \beta_{LM}$$

where $$W^{\pm}_{\ell L \ell'} = \pm 2 \xi^{\mp} P^{\mp}_{\ell L \ell'} \sqrt{\frac{(2\ell+1)(2L+1)(2\ell'+1)}{4\pi}} \begin{pmatrix} \ell & L & \ell' \\ -2 & 0 & 2 \end{pmatrix}$$

and parity indicators $$\xi^{+} = 1 \; , \; \xi^{-} = i$$

$$P^{\pm}_{\ell L \ell'} = \frac{1 \pm (-1)^{\ell+L+\ell'}}{2}$$

Anisotropic birefringence produces a similar mode mixing than gravitational lensing but

* gravitational lensing conserves parity, thus it doesn't introduce an ensemble-averaged $\langle EB \rangle$ even though it produces B modes from the convolution of E and the lensing potential
* starting from pure E polarization
  - lensing induces B modes for $\ell + L + \ell' = \text{odd}$
  - $\beta(\hat{n})$ induces B modes for $\ell + L + \ell' = \text{even}$

  Thus these effects are orthogonal (at linear order) and can be distinguished geometrically on the full sky. Gluscevic+ 2009 [arXiv: 0905.1687]

The birefringence field can be reconstructed through quadratic estimators

$$\beta_{LM} = A_L \sum_{\ell \ell'} \begin{pmatrix} \ell & \ell' & L \\ m & m' & M \end{pmatrix} f_{\ell L \ell'} \hat{e}^{obs}_{\ell m} \hat{b}^{obs}_{\ell' m'}$$

Kernel $f_{\ell L \ell'} = -W^{-}_{\ell' L \ell} C_\ell^{EE}$

$\hat{e}^{obs}_{\ell m}$, $\hat{b}^{obs}_{\ell m}$: inverse-variance filtered, i.e., $\frac{x^{obs}_{\ell m}}{C_\ell^{xx} + N_\ell}$ if diagonal in harmonic space

Normalization $A_L = \frac{1}{2L+1} \sum_{\ell \ell'} \frac{(f_{\ell L \ell'})^2}{\hat{C}_\ell^{EE} \hat{C}_{\ell'}^{BB}}$

Namikawa+ 2020 [arXiv: 2210.08038]

Current constraints) BICEP $A_{CB} = \frac{L(L+1)}{2\pi} C_L^{BB} \leq 0.044 \times 10^{-4}$ [rad^2] (95% CL)

BICEP/Keck Collaboration 2023 [arXiv: 2210.08038]

4.3 Radio galaxies

Radio galaxies with extended jets of synchrotron radiation

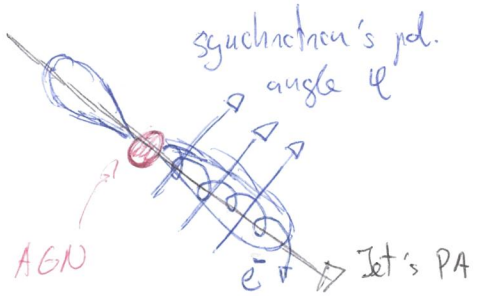

Synchrotron radiation is linearly polarized and expected to form $\approx 90°$ with the direction of the jet

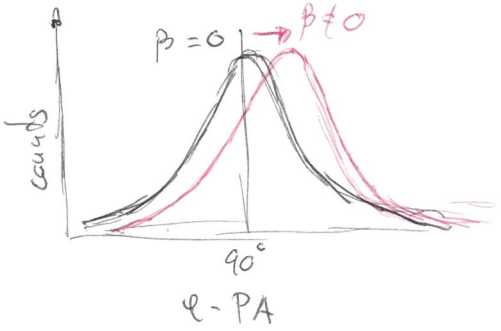

Find $\beta \neq 0$ as a shift from 90^c in the statistics of ψ-PA from a large-enough sample of radio galaxies Carelli + 1990

We can measure $\beta(z)$ by taking a tomographic approach and grouping radio galaxies into redshift bins. We will need $O(10^5 - 10^6)$ polarized radio galaxies up to $z \lesssim 2$ to distinguish between axion DE and DM, which is doable with upcoming surveys like ASKAP or SKA

Naokawa 2025 [arXiv: 2504.06709]

4.4 Protoplanetary disk

Flattened gas cloud surrounding a young star, where planets are thought to be formed, that scatters the central star's light at optical and near-infrared wavelengths.

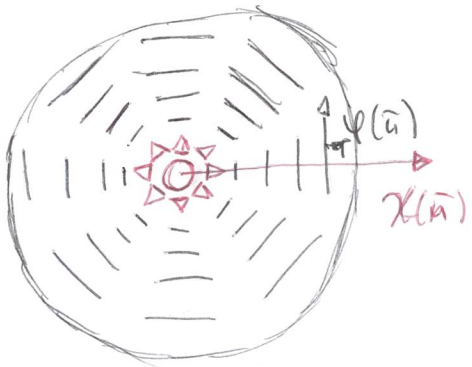

The protoplanetary disk emission is linearly polarized perpendicular to the radial direction from the star.

A systematic shift on the $\psi - \chi$ distribution will indicate $\beta \neq 0$

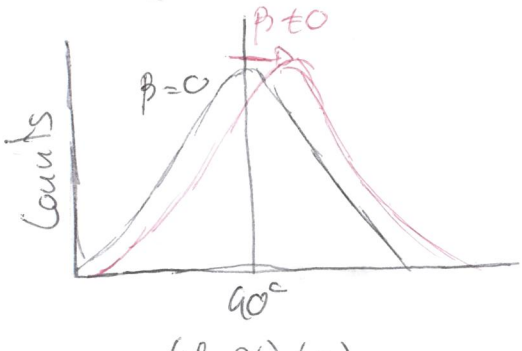

Fujita+ 2019 [arXiv: 1811.03525]

4.5 Time delays between strongly lensed images

Basu + 2021 [arXiv: 2007.01440]

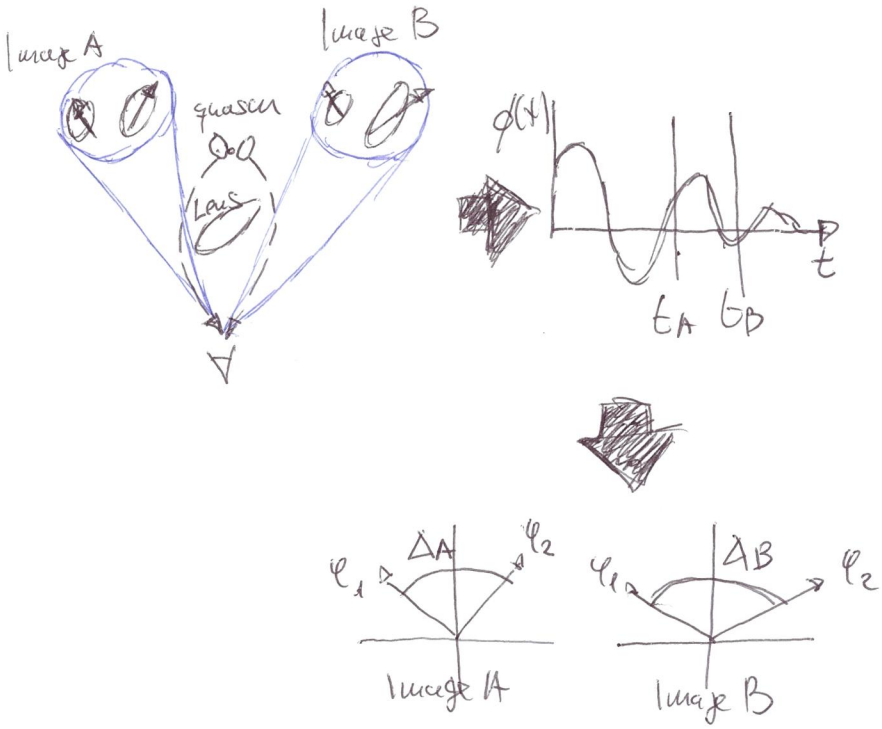

$\Delta = \Delta_A - \Delta_B$ contains information about the oscillations of $\phi(t)$ at the source

We observe the multiple lensed images of a polarized quasar at different times

As the photons from each image travel a different optical path, they would have experienced a different birefringence rotation

We don't need to know the intrinsic polarization angle as we can search for relative differences between multiple images

4.6 Black hole polarimetry

Axions are expected to form a dense cloud near the event horizon through the superradiance mechanism.

The linearly polarized photons emitted from the innermost region of the accretion disk, lying inside such dense cloud, will experience a birefringence rotation that makes their position angle oscillate in time with a period equal to the $\phi(t)$ at the source.

Polarimetric images of supermassive black holes from the Event Horizon Telescope could detect this effect Chen + 2020 [arXiv: 1905.02213]

4.7 Pulsars

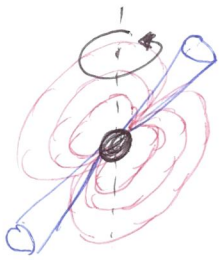

Highly magnetized rotating neutron stars that emit beams of electromagnetic radiation out of its magnetic poles. The pulses are extraordinarily regular, with periods ranging from milliseconds to seconds.

Use the radio emission of pulsars measured by pulsar timing arrays to search for a periodic birefringence rotation induced in the PA of pulses by the axion field Castillo + 2022 [arXiv: 2201.03422]

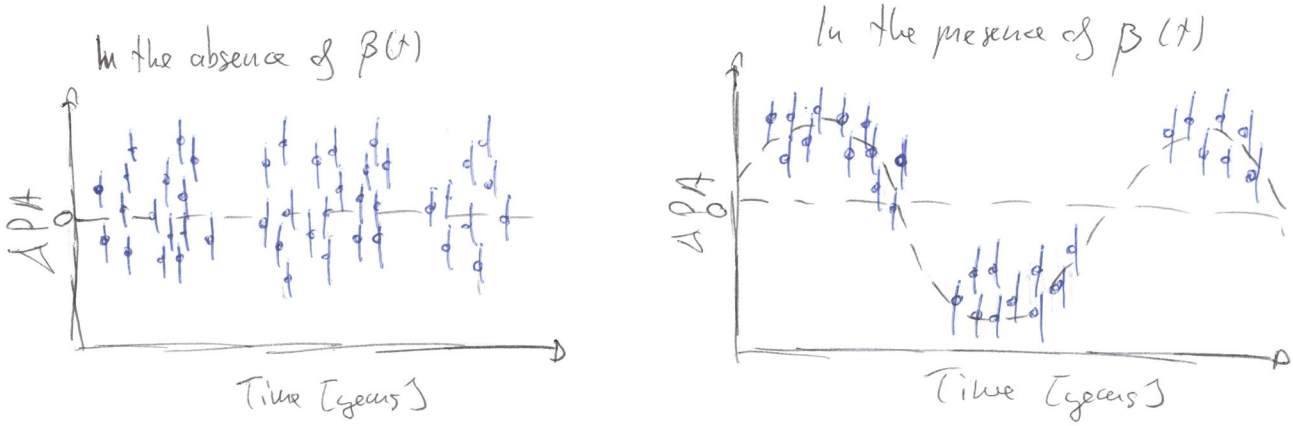

CMB experiments frequently observe the Crab Nebula (supernova remnant + pulsar wind nebula), a.k.a. Tau A, to use its emission as a reference source for calibration since it is one of the brightest compact sources of synchrotron radiation in the microwave sky.

Recently POLARBEAR found a 2.5 σ limit of $\beta(t)$ with oscillation periods of 61 and 52 days, corresponding to 7.8×10^{-22} eV and 9.2×10^{-22} eV masses, by looking for a change in PA across Tau A maps obtained at different observation times. Adachi + 2024 [arXiv: 2403.02096]

Pulsar timing arrays can be used to detect the temporal and spatial variations of the position angle and constraint axions

↳ Dubbed as pulsar polarization arrays

Liu + 2023 [arXiv: 2111.10615]

4.8 Laboratory experiments

Optical interferometry provides high-accuracy measurements of tiny deviations in the phase velocity of laser beams
We can use interferometry to measure the phase velocity difference that birefringence introduces between left- and right-handed circular polarization states.

Resonant ring cavity consisting of four mirrors

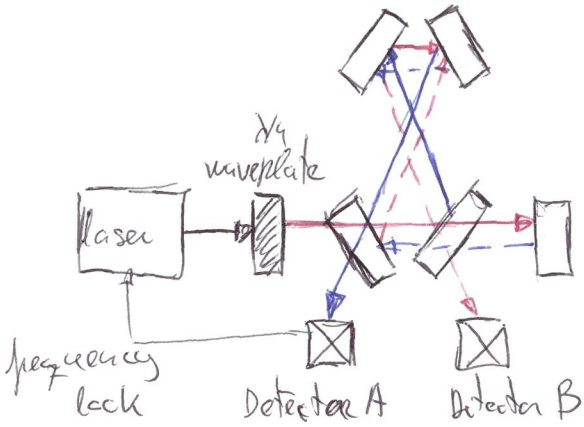

— forward beam in solid lines
--- reflected beam in dashed lines
— left handed
— right handed
} Each reflection on a mirror changes the circular polarization of the beam

Detector A is used to lock the laser frequency of the resonant cavity
Detector B monitors the modulation of the resonant frequency difference of the two optical paths

Experiments such as DANCE Obata + 2018 [arXiv: 1805.11753]
Michimura + 2020 [arXiv: 1911.05186]
LIDA Heinze + 2024 [arXiv: 2307.01365]
ADBC Pandey + 2024 [arXiv: 2404.17517]

OR
Install special optics into gravitational wave interferometers to make them sensitive to axion birefringence

Recently installed in KAGRA Michimura + 2021 [arXiv: 2111.04420]

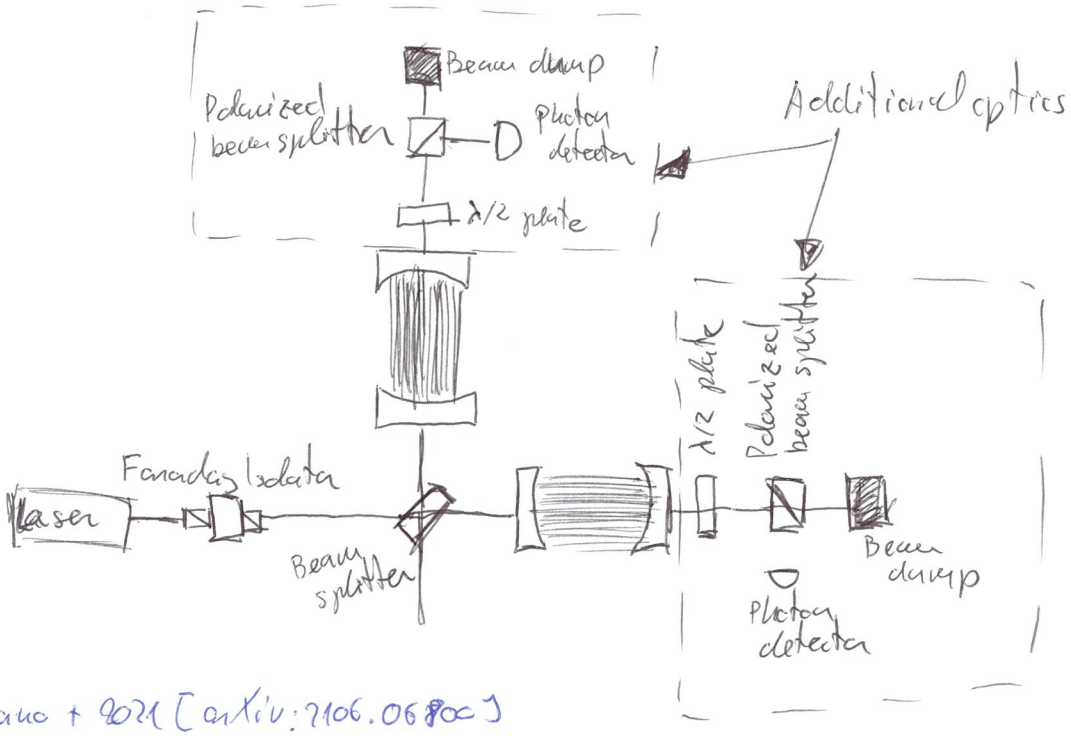

Nagano + 2021 [arXiv: 2106.08800]